



## Galactic and Anomalous Cosmic Rays in the Heliosphere

A. C. CUMMINGS

*Space Radiation Laboratory, California Institute of Technology, Pasadena CA 91125 USA*

*ace@srl.caltech.edu*

**Abstract.** The contributions to the sessions SH 3.1-3.5, SH 4, SH 5, and one paper from SH 2.1 of the 30th International Cosmic Ray Conference are summarized. Only the 83 contributions that were presented orally or in poster form are reviewed.

### Introduction

In this report the presented contributions of sessions SH 3.1-3.5, SH 4, SH 5, and one paper from SH 2.1 are reviewed. The topics covered are galactic cosmic rays (GCRs) in the heliosphere, anomalous cosmic rays (ACRs) in the heliosphere, and cosmic rays at the termination shock and in the heliosheath. Most of the phenomena addressed in these sections are governed by the Parker transport equation for cosmic rays [1] with the addition of a source term and a term to account for second order Fermi acceleration, also known as stochastic acceleration. This equation, with the additions mentioned, provides a mathematical description of the transport of cosmic rays, both anomalous and galactic, from their source to the point of observation through the processes of diffusion, convection, adiabatic energy change, and drift motions in the large-scale interplanetary magnetic field (IMF). The interplay of these effects is complex and time-dependent on many time scales. Many of the studies seek to better quantify the parameters in the transport equation or to learn more about the source region, e.g., of anomalous cosmic rays. Other studies look back in time for thousands of years and bring to light interesting trends and periodicities, some of which relate to long-term changes in the magnetic field of the Sun.

Based on the content of the presentations, the discussion in this report is organized around 10 topics. One of these is termed "Not\_SH", as it involves phenomena at such high energy as to not be particularly relevant to the heliosphere. However,

this topic did produce one of the more interesting controversies and is retained in this review. The remaining topics, in shorthand notation and in the order discussed, are "New\_capability", "Oddlot", "Mod\_model\_emp", "Mod\_model", "Diff\_coeff", "Rad\_grad", "Period\_long", "Period\_short", and "Near\_TS".

### Not\_SH

There were four papers in this category. The Tibet air shower array group [4] analyzed  $\sim 37$  billion air shower events from November 1999 to October 2005 and report that the region of maximum excess and the region of maximum deficit on the celestial sky are not  $180^\circ$  apart. Other groups report a similar result for cosmic rays of  $\sim 3$  TeV [5] and  $\sim 10$  TeV [6]. The Tibet group suggests that the best fit to the observations is a superposition of a bi-directional flow and a unidirectional flow of GCRs. They hypothesize that the solar system is rather near the edge of the local interstellar cloud (LIC) and that the density of cosmic rays is greater outside than inside the LIC. Further, they suppose that an interstellar magnetic field line that crosses the heliosphere would connect to the edge of the LIC in both directions, producing a bi-directional flow of cosmic rays towards the Earth. A unidirectional flow would be perpendicular to the bi-directional flow due to the  $\mathbf{B} \times \nabla N$  drift effect. They then deduce the orientation of the local interstellar magnetic field, as well as its polarity, and, as shown in Fig. 1, find that the direction agrees

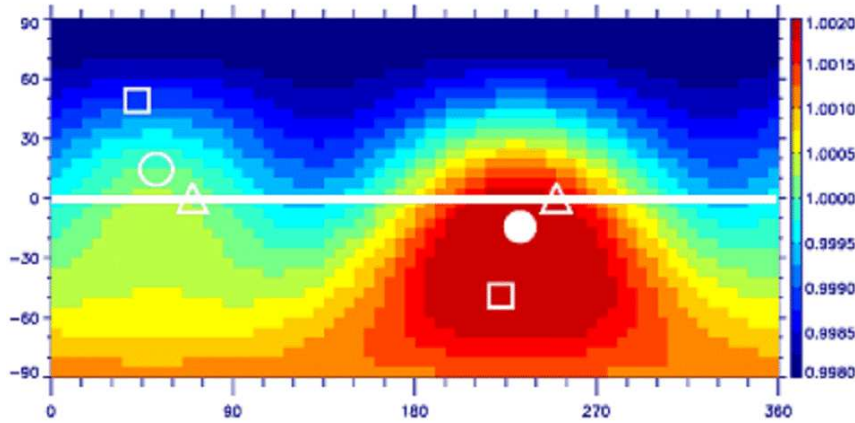


Fig. 1. The best-fit in Galactic coordinates of the sidereal anisotropy of  $\sim 5$  TeV cosmic ray intensity. Full (open) circle represents the direction parallel (anti-parallel) to the local interstellar magnetic field (LISMF). Squares and triangles show the LISMF orientations by Lallement et al. [2] and Frisch [3], respectively. From Amenomori et al. [4].

better with the Frisch estimate [3] than the one by Lallement [2].

Lidvansky et al. [7] dispute this interpretation and claim that the declination and source amplitude cannot be determined from observations which normalize the average intensity in each declination band to unity, which is the way the measurements by all the groups were done. They develop a method to properly deduce the declination and source amplitude and apply it to their BUST underground array data ( $\sim 2.5$  TeV) and find that there is one sidereal wave with the regions of excess and deficit  $180^\circ$  apart. This disagreement was not resolved at this conference.

### New capability

There were nine presentations in this category. The topics addressed ranged from new instruments, proposed new instruments, new capabilities of existing instruments, and new data bases.

IBEX-Lo was discussed by Möbius et al. [9]. It is a new instrument to be launched next year to measure energetic neutrals from charge-exchange of hot ions in the heliosheath with interstellar neutrals. It will have a new triple-coincidence system which should make for a big improvement over previous energetic neutral particle instruments.

CALET [10] is a proposed cosmic ray electron and gamma-ray instrument for the Space Station, and GOSAT [11] is a new mission that will

launch next year into a near-polar Earth orbit and will have a comprehensive set of low-energy particle detectors on board.

Capabilities of the PAMELA experiment were discussed [12]. PAMELA was launched 15 June 2006 into a highly-inclined low-Earth orbit. It can measure protons, antiprotons, positrons, electrons, and nuclei to quite high energies (hundreds of GeV) and will be able to measure the high energy portion of solar energetic particle events. Work has begun on analyzing data from the December 2006 solar events. Also working on data from the same solar events is the ARGO-YBJ air shower array team [13]. They have introduced a new scaler mode that allows studies down to a few GeV.

De Nolfo et al. [14] have made new estimates of the detection efficiency of He nuclei in the ACE/CRIS instrument, which should open up some new studies and allow those data to be distributed to the community. And Krainev [15] proposes to upgrade the electronics for the regular balloon monitoring program to allow the recording of the pulse waveform.

Two new data bases were discussed. One, the interactive data base of cosmic ray anisotropy [16], is online now. It contains information on anisotropy from the GSM network of 60 neutron monitors. The other is VICRO (Virtual Cosmic Ray Observatory) [17] which is in the development stage. It will contain data from the heliospheric

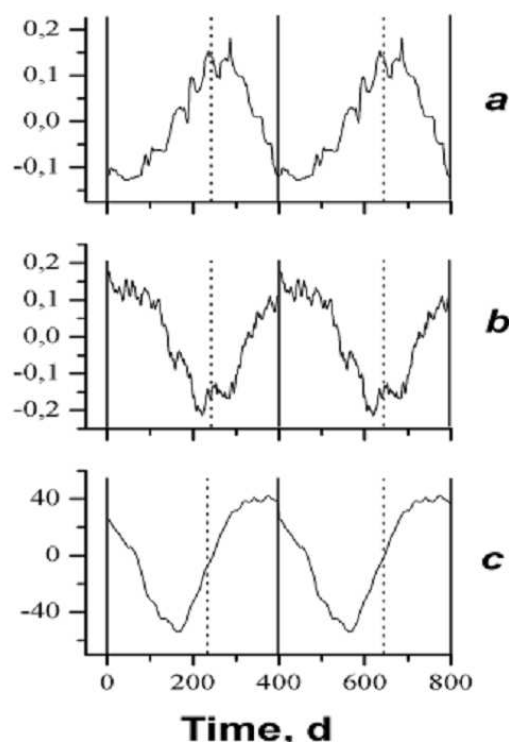


Fig. 2. Superposition of data for the 399 day Jupiter-Earth synodic period after filtering. The vertical solid lines correspond to the opposition times of the Earth and Jupiter; the dashed lines correspond to the times Earth crosses the interplanetary magnetic field (IMF) connecting Jupiter and the Sun. a) electron intensity. b) IMF magnitude. c) Oulu neutron monitor data. From Timofeev et al. [8].

network of spacecraft as well as data from balloon experiments and neutron monitors.

### Oddlot

There were five presentations in this category. These papers discussed one of a kind topics not easily combined with others. One of these described the ALTCRISS project [25] to measure the radiation environment on the Space Station. Another described measurements of ions in Earth's radiation belts [26] using data from the TSUBASA satellite. The authors claim that their results are in reasonable agreement with previous studies. Another [27] reported the vertical muon flux at 5.3 GV cutoff at ground level and at 25 m water equivalent for 2002-2006.

Timofeev et al. [8] find that the 2-12 MeV electron intensity from the IMP-8 spacecraft, the in-

terplanetary magnetic field (IMF) magnitude, and the Oulu neutron monitor rate all exhibit a 399-day periodicity, which is the synodic period of Jupiter with Earth. Using a superposed epoch analysis they find that the maximum in the electron intensity and the minimum in the magnetic field magnitude occur when Earth and Jupiter are on the same nominal magnetic field line, whereas the neutron monitor minimum intensity is shifted by 75 days as shown in Fig. 2. They suggest that the intense flux of electrons from Jupiter modifies the IMF strength and in turn causes an effect on the GCR intensity near Earth.

Finally, as shown in Fig. 3, Berezhko and Tanev [19] use a self-consistent theory of diffusive shock acceleration and associated Alfvén wave growth to reproduce the energy spectrum of protons at a traveling interplanetary shock observed in 1978.

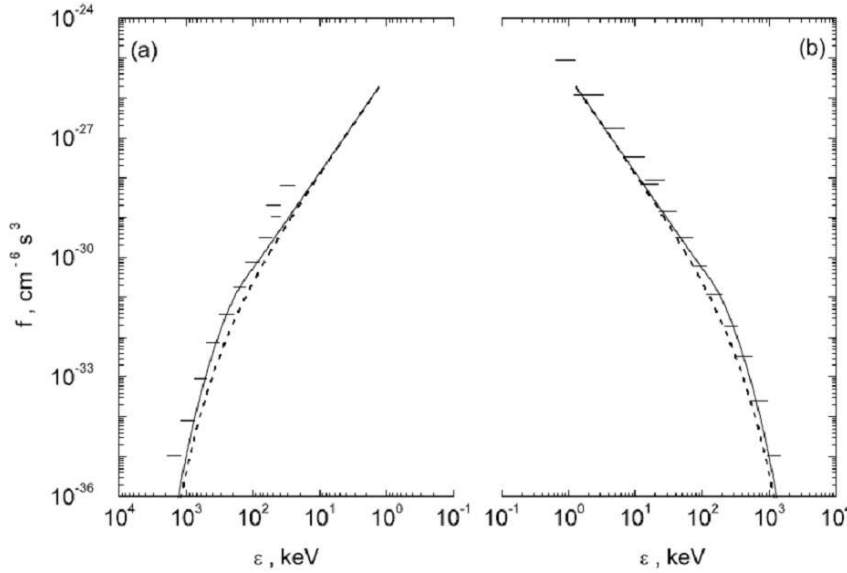


Fig. 3. Distribution function of accelerated protons as a function of their kinetic energy separately for protons moving toward the Sun (a) and away from the sun (b). Experimental data, obtained on August 26-27, 1978 by ISEE 3 [18] are shown as well. From Berezhko and Taneev [19].

### Mod model emp

There were three presentations in this category, which has to do with empirical models of modulation. Okhlopov and Stozhko [28] parameterized the regular balloon monitoring GCR intensity variations from 1957 to the present using indices based on a variety of solar activity parameters that vary every 10 years. Belov et al. [29] establish a new flare index to improve their semi-empirical model of the intensity of 10 GV GCRs vs. time near Earth. The class of the x-ray flare and the solar flare longitude relative to Earth figure into the new index.

Parameterizations of the energy spectra of GCR and ACR H and He at 1 AU have been done by Grimani et al. [30] for different phases of the solar cycle. The motivation was to develop a predictive tool for LISA, but these spectra would be of interest to a number of cosmic ray studies.

### Mod model

There were nine presentations in this category. Some of the papers in this section discuss modulation models and some discuss observations bear-

ing on parameters in modulation models. A good example of the latter are the papers by Mitchell et al. [31] and Clem et al. [23] which report on charge-sign dependent modulation effects in new proton/anti-proton measurements and new e<sup>+</sup>/e<sup>-</sup> measurements, respectively, as shown in Fig. 4. The anti-proton/proton effects are due to drifts in the large scale IMF and are consistent with the Bieber et al. model [21] but not the Moskalenko et al. model [32]. The e<sup>+</sup>/e<sup>-</sup> effects are consistent with the Clem et al. model [20].

Two 3D models [33, 34] of modulation used a modified Parker field, the so-called “Fisk-Parker hybrid field”, which is shown in Fig. 5. The authors were able to incorporate a latitude-dependent solar wind speed for the first time in such models. Hitge et al. [33] found that the latitude dependence of the solar wind speed is not very important and that the global modulation results are similar to those using a pure Parker field, in contrast to earlier 2D results [35].

Two models investigate the effects on drifts of the heliospheric current sheet (HCS) tilt (Usoskin et al. [36]) and of increasing turbulence (Minnie et al. [37]). Not surprisingly, as shown in Fig. 6, higher turbulence levels reduce the drift speed. The

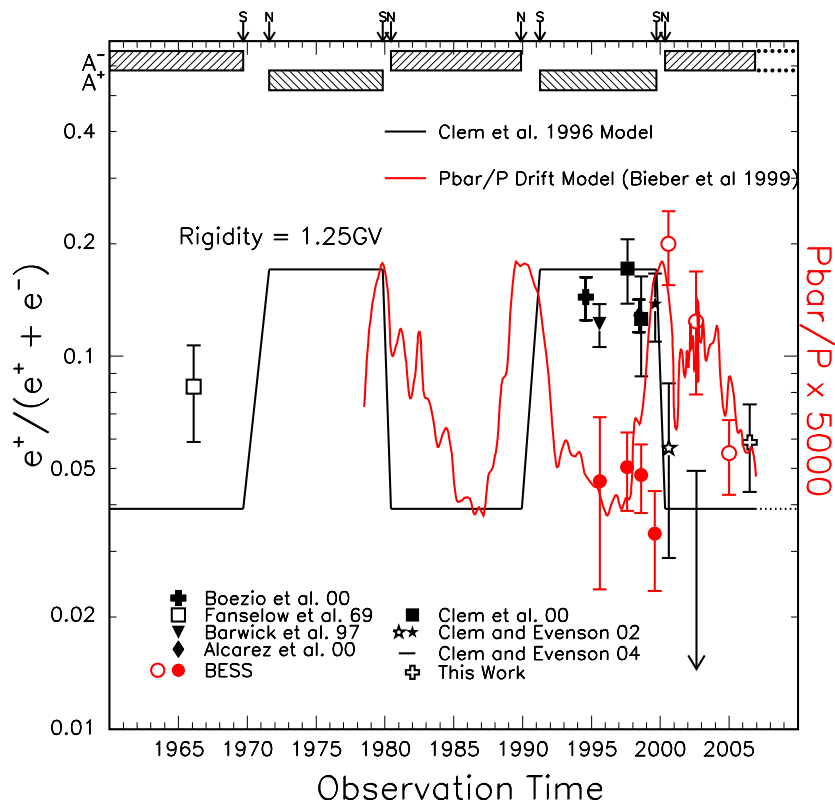


Fig. 4. Time profile of positron abundance (black) and anti-proton ratio (red) at a rigidity of roughly 1.3 GV. Solid symbols show data taken in the  $A > 0$  state, while the open symbols represent data taken in the  $A < 0$  state. Shaded rectangles represent periods of well defined magnetic polarity. The black line is a positron abundance prediction based on the analysis of Clem et al. [20]. The red line is an anti-proton/proton ratio drift (steady-state) model [21] interpolated to 1.3 GV. The current sheet tilt angles used in the drift model were acquired from the Wilcox Solar Observatory data base. Dashed lines represent the predicted results for future observations. The anti-protons were measured by the series of BESS flights [22] (and references therein). From Clem and Evenson [23]; see their paper for references in figure.

results may lead to revisions of modulation models in the way drift effects are suppressed. Rapid drift along the current sheet is washed out by increasing the tilt of the HCS [36]. However, drift effects in the large-scale IMF do remain at tilt angles up to at least 40 deg.

Bobik et al. [38] introduced a novel concept into their transport model: they allowed particles that escape the heliosphere to propagate in the interstellar medium and re-enter the heliosphere. For the parameters they used, they find about a 20% effect on the intensity of GCR H below a few GeV, as shown in Fig. 7.

### Diff\_coeff

There were eleven presentations in this category concerned with diffusion coefficients. There were several new developments. Shalchi et al. [39] found that they could reproduce the Palmer consensus [40] for the parallel and perpendicular mean free pathlength using a new NADT turbulence model in combination with QLT for parallel diffusion and NLGC for perpendicular diffusion (see, e.g., Fig. 8). Going one step beyond that for perpendicular diffusion, Shalchi and Kourakis [41] presented a new, improved theoretical treatment of the perpendicular transport of cosmic rays, called the Generalized Compound Diffusion model. The

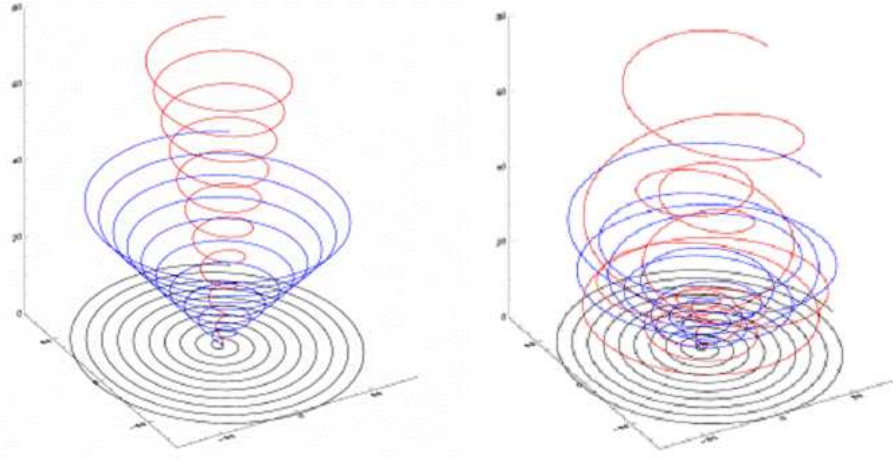


Fig. 5. The Parker IMF configuration model (left) and the Fisk-Parker hybrid IMF configuration model from Sternal et al. [24].

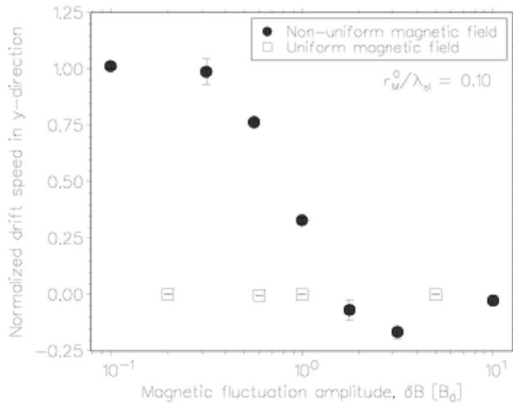


Fig. 6. Simulated drift speed  $v_D$  normalized to the weak scattering value  $v_D^{ws}$  as a function of the magnetic fluctuation amplitude  $\delta B$ , in units of the magnitude of the background magnetic field  $B_0$ . From Minnie et al. [37].

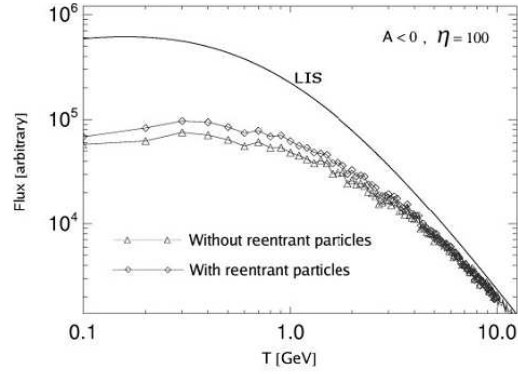


Fig. 7. Modulated galactic cosmic ray proton spectra at 1 AU and for  $\eta = 100$ , where  $\eta$  is the ratio of the mean free path to the Larmour radius, together with a local interstellar spectrum. Line with triangles denotes a spectrum without reentrant particles and line with diamonds denotes a spectrum with reentrant particles. From Bobik et al. [38].

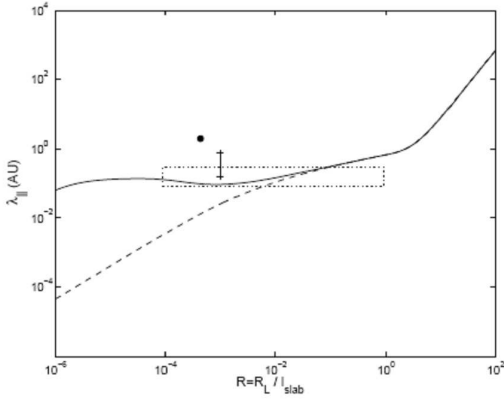


Fig. 8. The parallel mean free path  $\lambda_{||}$  versus  $R = R_L / l_{slab}$  ( $R_L$  = Larmour-radius,  $l_{slab}$  = slab bendover scale) obtained with the NADT-model. Shown are QLT results for electrons (solid line) and protons (dashed line) in comparison with the Palmer consensus (Palmer [40], box), Ulysses observations (Gloeckler et al. [42], dot), and AMPTE spacecraft observations (Möbius et al. [43], vertical line). From Shalchi et al. [39].

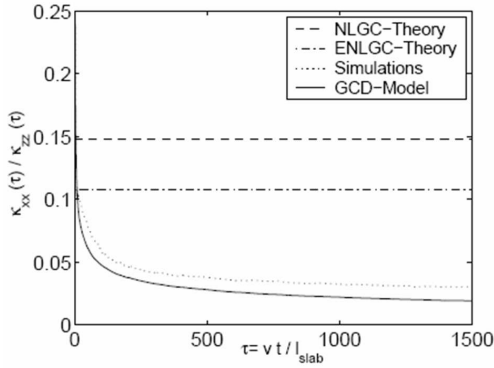


Fig. 9. The ratio of perpendicular and parallel diffusion coefficients ( $\kappa_{xx}(t) / \kappa_{zz}(t)$ ) for  $R = R_L / l_{slab} = 0.001$ . The results from test-particle simulations (dotted line) are compared to various theoretical results: NLGC-theory (dashed line), ENLGC-theory (dash-dotted line), and our GCD-model (solid line). From Shalchi and Kourakis [41].

results agree better with simulations than previous theories, as shown in Fig. 9.

Useful for investigating 2D vs. slab turbulence is the study by Dasso et al. [44] wherein magnetic field correlations done on one spacecraft at two different times are compared with correlations done on two spacecraft at the same time.

Alania et al. [45] find that 75-80% of the amplitude of the 11-year GCR intensity variation is caused by IMF turbulence variations. They find they can estimate the magnetic turbulence power spectrum index in the  $10^{-6}$  to  $10^{-5}$  Hz frequency range from the power-law index of the rigidity dependence of neutron monitor intensity variations.

In other developments, Nkosi et al. [46] point out that strong anisotropies of Jovian electrons off the equatorial plane can be used to study perpendicular diffusion. Burger and Englebrecht [47] used a Fisk-Parker hybrid field and a recent version of the perpendicular diffusion mean-free path-length to explain the amplitude of recurrent 26-day variations being larger in  $A > 0$  than in  $A < 0$  periods for both low and high rigidities. Sternal et al. [24] compare diffusion tensors in a Parker field vs. a Fisk-Parker hybrid field and find that the Fisk-Parker hybrid field can at least partly explain enhanced latitudinal transport. They concede, however, that it's not the only possible explanation.

## Rad\_grad

There were six presentations in this category. This topic, radial gradients, is potentially closely related to diffusion coefficients, since in simple 1D models, in the rigidity range where diffusion and convective effects dominate adiabatic energy change effects, the gradient is inversely proportional to the diffusion coefficient. For  $\sim 175$  MeV GCR H and  $\sim 270$  MeV/nuc GCR He, Morales-Olivares and Caballero-Lopez [48] find that at solar maximum for radial distances inside 40 AU, adiabatic deceleration dominates and results in a lower radial gradient than beyond 40 AU where diffusion and convection are dominant. The values of the radial gradient are in the few percent per AU range and agree fairly well with estimates from Gieseler et al. [49] and one that can be derived from Krainev and Kalinin [50] observations at similar energies. Leske et al. [51] report on ACR O gradients and find them to be sensitive to the polarity cycle of the Sun's magnetic field and to the tilt angle of the HCS.

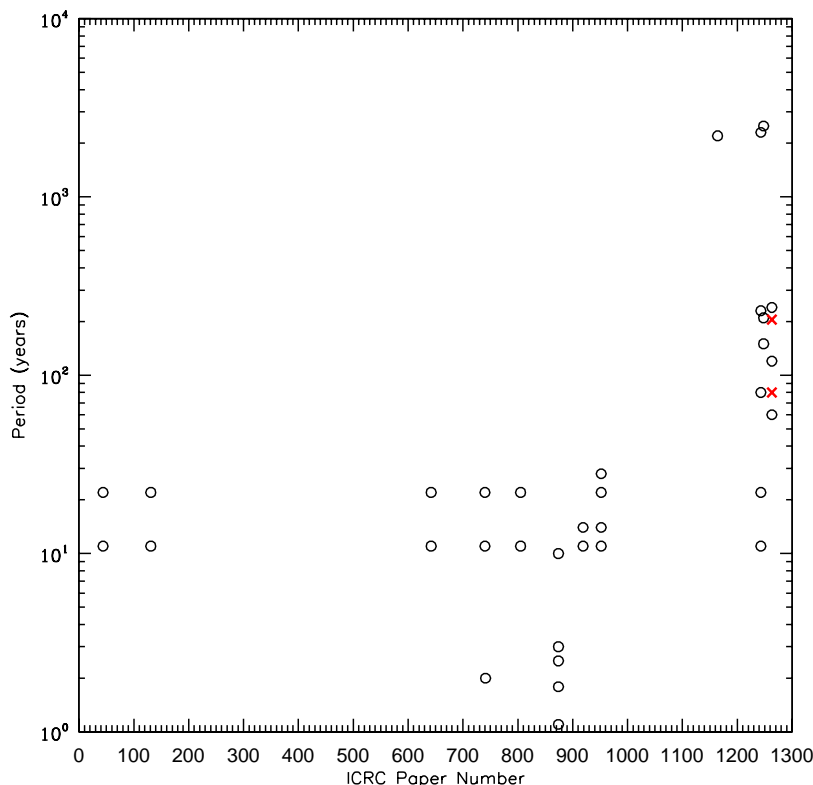


Fig. 10. Period of cosmic ray intensity variations vs. ICRC paper number as reported at this ICRC. The two red x symbols indicate periodicities of  $\sim 80$  years and 205 years, previously reported in the literature, that were found not to exist by Velasco et al. [52].

## Period long

There were fifteen presentations in this category, which was the most of any category. As seen in Fig. 10, there were a great many different periodicities discussed. Perhaps the two most intriguing are the ones denoted by an “x”, which are long-standing periodicities, the 80-90-year Gleissberg cycle and the 205-year de Vries cycle, which were not found when using the latest wavelet method of analysis. Velasco et al. [52] suggest the the previous results were faulty because they used the Fourier transform technique on non-stationary data. Instead, they find significant periodicities of 60 years, 120 years, and 240 years. These and other longer periods reported in this conference relate to changes of the Sun’s magnetic field.

McCracken [53] estimated the strength of the heliomagnetic field over the last 600 years based on a pseudo-Climax neutron monitor rate derived from cosmogenic  $^{10}\text{Be}$  data prior to 1933 and instrumental records since then. The results are shown in Fig. 11. Apparently, we live in a time of relatively low GCR intensity, but that could change.

Many studies find the  $\sim 11$  year and  $\sim 22$  year periodicities, which are related to the 11-year solar activity cycle and the Sun’s magnetic field reversal each 11 years. The field reversal changes the drift patterns in the heliosphere and results in a 22-year periodicity in the intensity of cosmic rays. In the few-year periodicity regime, Laurenza et al. [54] find periodicities of 2-3 years that are thought to relate to photospheric field modes of oscillation. de Caso et al. [55] examine several solar indices



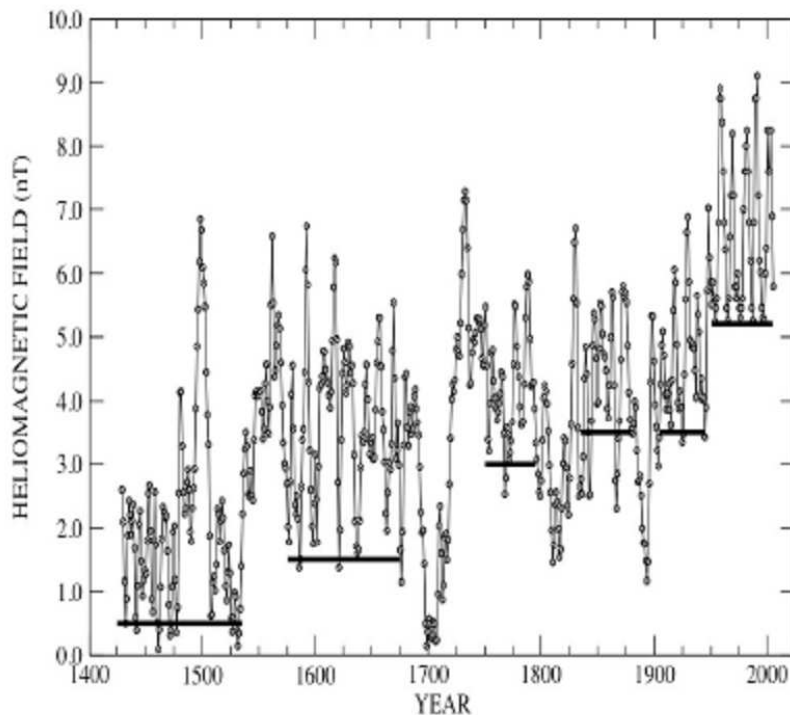


Fig. 11. The estimated heliomagnetic field, 1428-2005, based on the data in Fig. 1 of McCracken [53]. The data are annual estimates, passed through a 1,4,6,4,1 binomial filter. From McCracken [53].

and find a 2-year periodicity that hints of a double solar dynamo.

### Period\_short

There were nine presentations in this category, which are concerned with periodicities of order 1 year or shorter. In this conference, tri-diurnal and quart-diurnal variations at neutron monitor energies were characterized by Richharia and co-workers [56, 57]. Explanations of these three and four times daily variations were not offered.

Modzelewska and Alania [58] attribute 27-day variations of GCR anisotropy at neutron monitor energies during solar minimum to heliolongitude variations of the solar wind speed. They find the amplitudes and phases are more clearly established in the  $A > 0$  rather than the  $A < 0$  phases of the solar cycle.

At higher, multi-TeV air shower energies, Li et al. [59] find three, and only three, periodicities in the periodicity range from 1 hour to 2 years: a so-

lar diurnal variation due to the Compton-Getting effect of the Earth's orbital motion, a sidereal diurnal variation, and a sidereal semi-diurnal variation.

One wrinkle in the high-energy anisotropy is that after correcting for the 0.04% solar diurnal Compton-Getting anisotropy, there is a residual anisotropy of about the same magnitude. This was found in the 4 TeV data from the Tibet air shower array [60] and for solar maximum only in the  $\sim 600$  GeV Matshushiro underground muon telescope data reported by Kóta et al. [61]. Kóta et al. offer an explanation for the latter based on a trajectory tracing study when the heliospheric current sheet is highly inclined.

### Near\_TS

There were twelve presentations in this category. The major news in this category was delivered on 16 December 2004 when Voyager 1 crossed the solar wind termination shock. One of the major puzzles of that crossing was that the ACR He energy

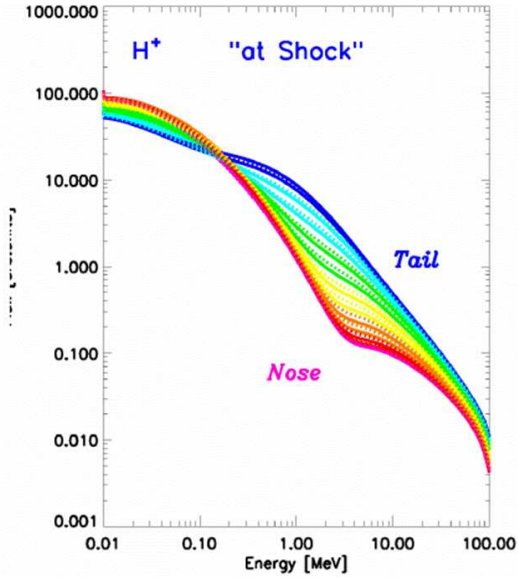


Fig. 12. Variation of the energy spectrum along the blunt termination shock. The modulated spectrum at the nose (red) gradually unfolds toward the tail (blue). From Kóta [61].

spectrum did not unfold to its expected power-law shape at low energies but instead remained essentially unchanged, although the spectrum did start to unroll later. Three theories to explain this phenomenon were discussed at this conference.

The first was the theory that ACRs are preferentially accelerated along the flanks or tail of the termination shock [62, 5]. Fig. 12 shows energy spectra of ACR H at different longitudinal positions of a blunt shock that support that point of view [5].

Ferreira et al. [63] and Moraal et al. [64] find that stochastic acceleration in the heliosheath could explain the observations. Fig. 13 shows the evolution of the ACR He energy spectrum expected in the heliosheath along the trajectory of V1 from the model of Ferreira et al.

Finally, Cummings and Stone [67] point out that according to recent calculations by Florinski and Zank [68], the energy spectrum at the termination shock could be disturbed from its nominal shape by merged interaction regions (MIRs). Jokipii and Giacalone [69] also note that the spectral disturbance could result from just the motion of the shock itself. A multi-year long train of MIRs was present at V2 prior to and after the crossing,

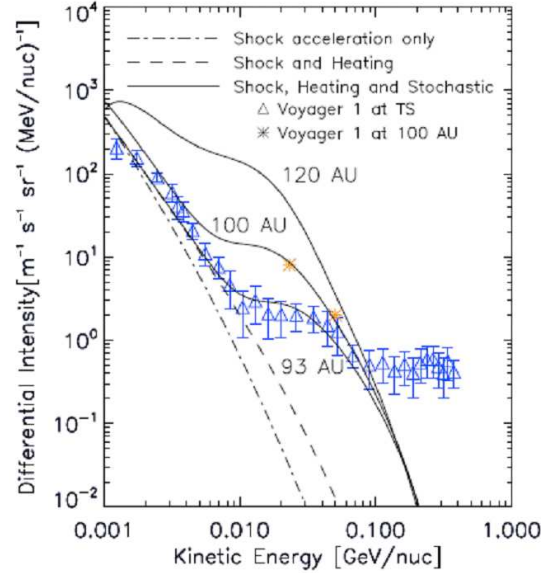


Fig. 13. Computed spectra for singly-ionized anomalous He at the termination shock (93 AU) for three acceleration scenarios: (1) diffusive shock acceleration only (dashed-dotted line), (2) diffusive shock acceleration and adiabatic heating (dashed line) and (3) shock acceleration, heating in the inner heliosheath, and acceleration of a stochastic nature (solid lines). The latter scenario is shown at the shock (bottom solid line), at 100 AU, and at 120 AU (top solid line). In comparison the observed Voyager 1 spectra at the observed termination shock are shown as the triangles [65, 66]. Also shown by the asterisk symbols are Voyager 1 observations at 100 AU (<http://voyager.gsfc.nasa.gov>). From Ferreira et al. [63].

mostly ending by mid-2004. Similar MIRs were likely present near the vicinity of V1. Furthermore, Cummings and Stone [67] point out that the ACR He spectrum evolved similarly at both V1 and V2 after the V1 shock crossing, indicating that the evolution was a temporal, not a spatial effect. The energy spectra at both spacecraft from 2004/209 to 2006/260 are shown in Figs. 14 and 15.

Also shown in Figs. 14 and 15 is a remarkable scaling among the spectra of H, He, and O from  $\sim 3$  MeV/nuc He to  $\sim 70$  MeV/nuc He. The H and O spectra in all panels have been multiplied by one factor in energy/nuc, 5.0 for O and 0.2 for H, and one factor in intensity, 1.4 for O and 1.2 for H, before plotting. The excellent agreement of the spectra is attributed to the diffusion coefficient being proportional to  $\beta R^{1.4}$  and the particles being singly charged.

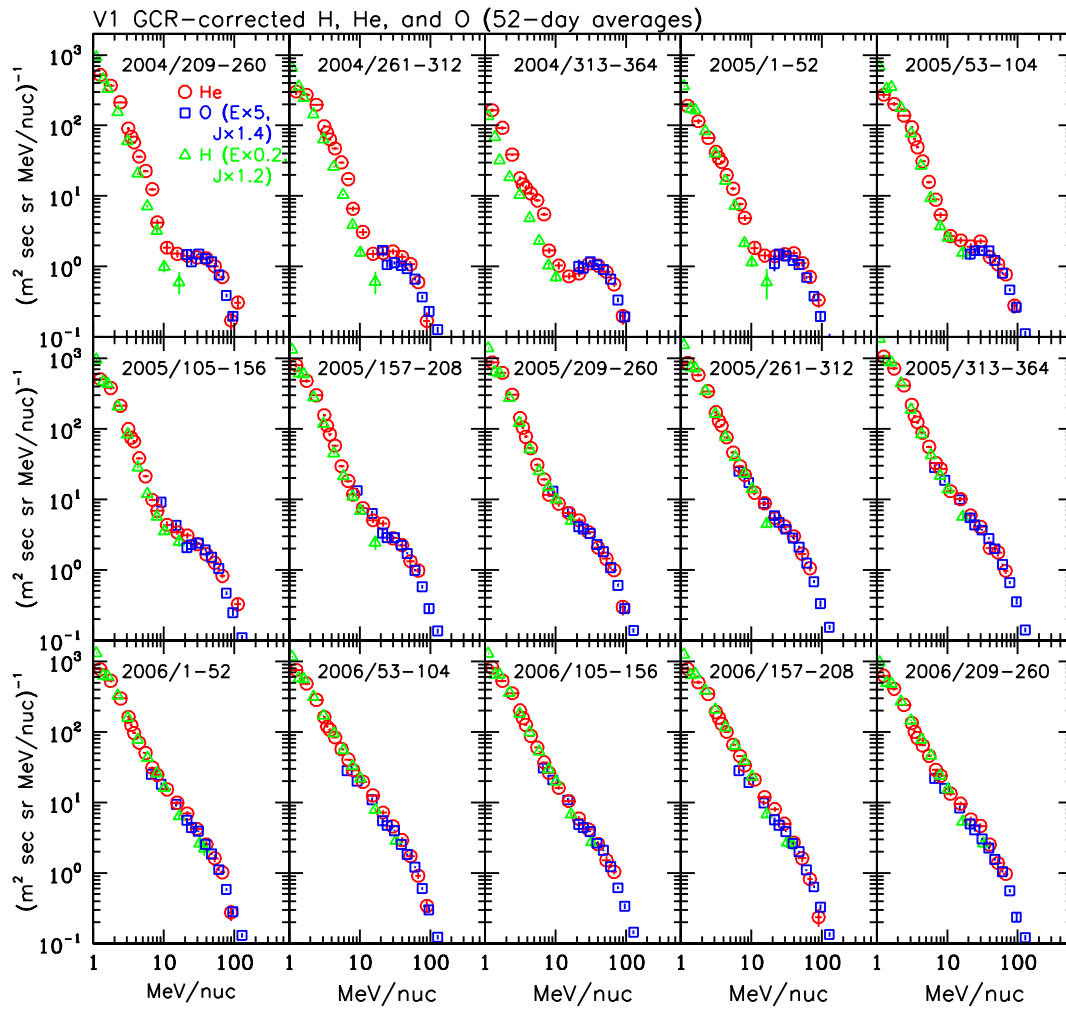


Fig. 14. Energy spectra of H, He, and O at V1 for fifteen 52-day periods. The observed spectra have been corrected for galactic cosmic rays (GCRs) based on the observed C energy spectrum. V1 crossed the shock on day 351 of 2004. The H and O energy spectra have been scaled by factors in energy/nuc and intensity as shown in the figure. From Cummings and Stone [67].

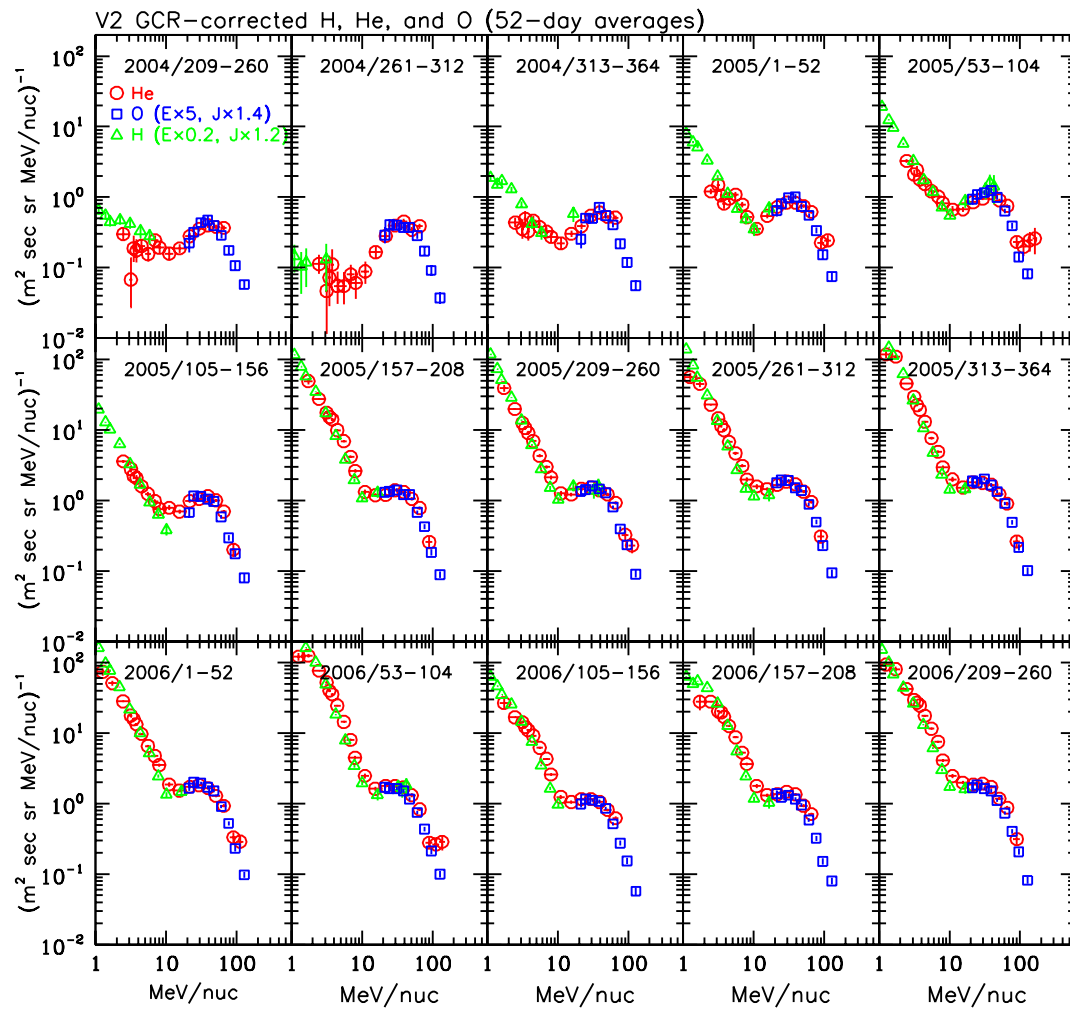


Fig. 15. Same as Fig. 14 except for V2. From Cummings and Stone [67].

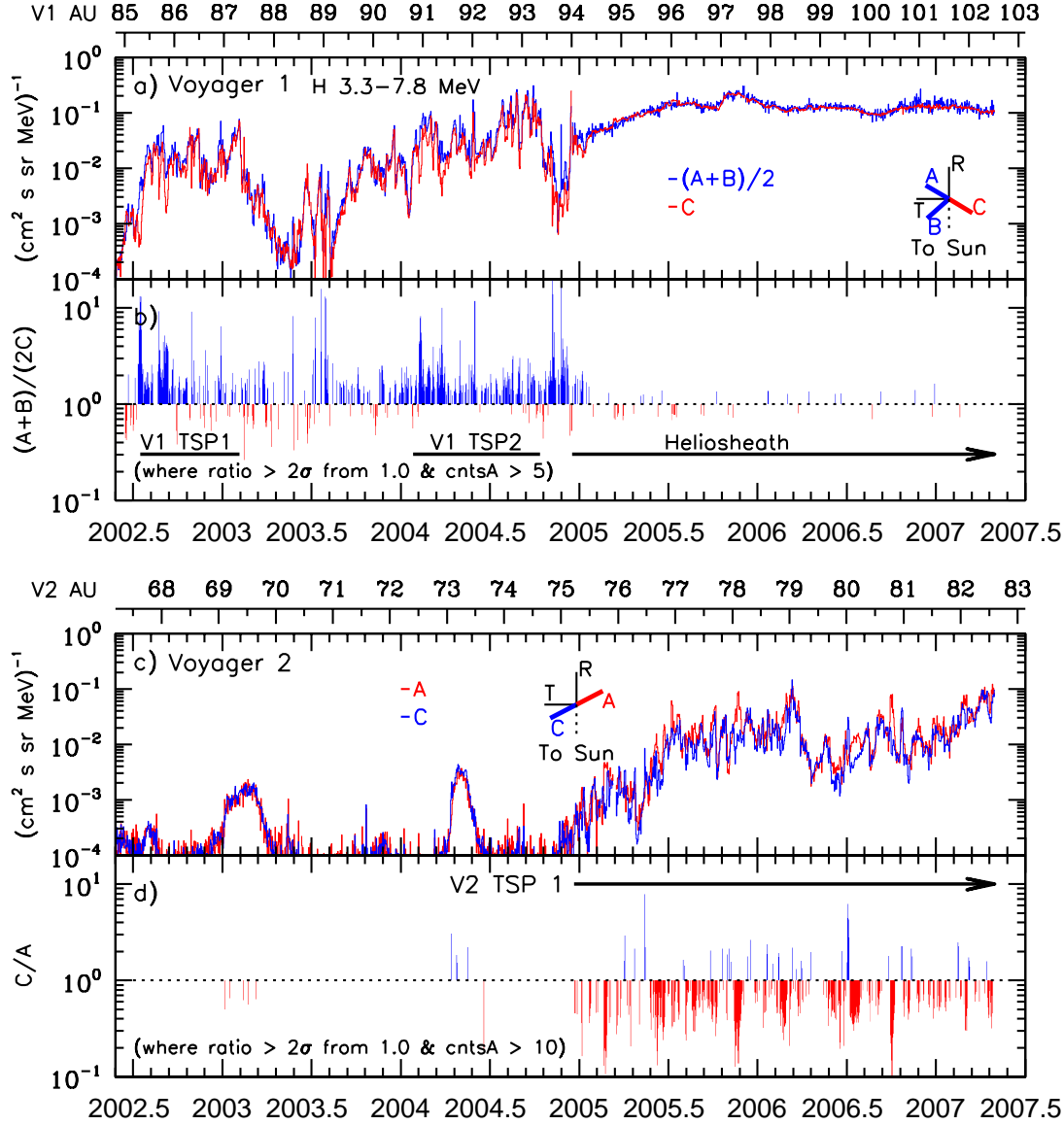


Fig. 16. Intensities and streaming of energetic H ions from the termination shock observed by Voyager 1 and Voyager 2. The observing directions of the Low Energy Telescopes A, B, and C, are shown in RTN coordinates with R radially outward and T in the azimuthal direction along the spiral magnetic field toward the Sun. Voyager 1 crossed the termination shock on 2004.96. As indicated by the ratio of outward vs. inward intensities, Voyager 1 began observing ions streaming outward from the shock along the interplanetary magnetic field in mid-2002 at 85 AU. Voyager 2 began observing upstream ions beaming inward along the field in late 2004 at 75 AU, indicating that the shock is likely closer in the southern hemisphere than at Voyager 1 in the north. From Stone et al. [70].

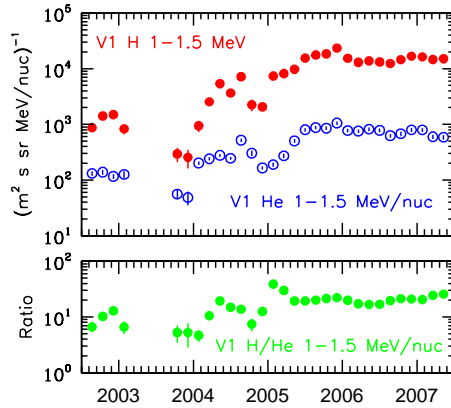


Fig. 17. The H and He intensities and the H/He ratio at 1-1.5 MeV/nuc (52-day averages). The ratio was smaller and more variable upstream of the shock than in the heliosheath. From Stone et al. [70].

Stone et al. [70] investigate the V1 H/He ratio at 1-1.5 MeV/nuc and find that the ratio is  $\sim 20$  from 2005-2007, as shown in Fig. 17, about 4 times higher than inferred from ACR studies at higher energies [71, 72], which implies that H pickup ions are more efficiently accelerated than was previously modeled. Energetic neutral atom (ENA) observations from SOHO also can reveal information about the ACRs and the structure of the heliosphere. Hilchenbach et al. [73] find more ENAs towards the tail region of the heliosphere than towards the nose. Czechowski et al. [74] also report on ENA measurements and find a discrepancy between the ENA H/He ratio as compared to the ACR H/He ratio. The discrepancy is by a factor of  $\sim 5$  and various possibilities were discussed to resolve the discrepancy but no conclusion was reached. They do find that the thickness of the heliosheath in the apex region, near where V1 and V2 are located, is  $\sim 20$ -30 AU, which would mean the Voyagers could reach it before running out of power in  $\sim 2020$ .

V2 is soon expected to cross the termination shock. This is evident from Fig. 16, which shows that the intensity of 3.3-7.8 H at V2 has reached the same level as that at V1 in the heliosheath. Further, the precursor beams of particles from the termination shock have been observed at V2 for about as long as they were at V1 prior to its crossing in December 2004.

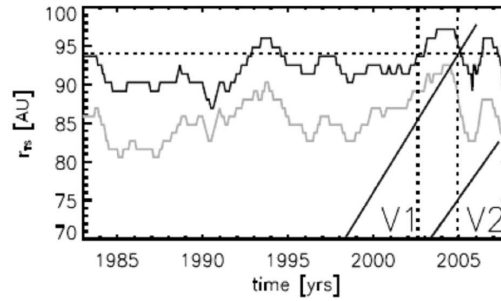


Fig. 18. The termination shock (TS) position as it varies with time, where it is assumed that Voyager 1 crossed the TS in 2004.9. The solid black line shows the TS position along Voyager 1's trajectory, while the grey line shows the TS position along the trajectory of Voyager 2. The dotted vertical lines correspond to 2002.6 and 2004.9, respectively, while the horizontal dotted line corresponds to 94 AU. From Snyman et al. [75].

A new calculation of the location of the termination shock in the vicinity of V2 was presented by Snyman et al. [75] and shown in Fig. 18. According to this model, V2 should cross the termination shock before this article is published.

## Summary

Much has been accomplished in this area of heliospheric physics in the last couple of years, much remains to be investigated, and there is much to look forward to with, e.g., the impending crossing of the termination shock by V2. Among the accomplishments that stand out is the work on perpendicular diffusion, which is reported at this conference to be a solved problem. If true, this would be a giant step forward in diffusion theory. Some negative progress may have also been made. For example, was the 80-90 year Gleissberg cycle a mistake and is an interpretation of the sidereal anisotropy at multi-TeV energies incorrect? Finally, will the V2 crossing of the solar wind termination shock resolve the mystery of where were the ACRs when V1 crossed? These and other questions will undoubtedly be debated over the next two years and reported on at the next international cosmic ray conference.

## Acknowledgements

This work was supported by NASA under contract NAS7-03001.

## References

- [1] E. N. Parker, *Planet. Space Sci.* 13 (1965) 9.
- [2] R. Lallement et al, *Science* 307 (2005) 1447.
- [3] P. C. Frisch, *Space Science Reviews* 78 (1996) 213.
- [4] The Tibet As $\gamma$  Collaboration, *Proceedings of 30th ICRC Merida, Mexico, (2007) Vol.1*, p. 593.
- [5] B. E. Kolterman et al, *Proceedings of 30th ICRC Merida, Mexico, (2007) Vol.1*, p. 617.
- [6] Y. Oyama et al, *Proceedings of 30th ICRC Merida, Mexico, (2007) Vol.1*, p. 605.
- [7] A. S. Lidvansky et al, *Proceedings of 30th ICRC Merida, Mexico, (2007) Vol.1*, p. 613.
- [8] V. E. Timofeev et al, *Proceedings of 30th ICRC Merida, Mexico, (2007) Vol.1*, p. 421.
- [9] E. Möbius et al, *Proceedings of 30th ICRC Merida, Mexico, (2007) Vol.1*, p. 841.
- [10] Y. Komori et al, *Proceedings of 30th ICRC Merida, Mexico, (2007) Vol.1*, p. 441.
- [11] Y. Sasaki et al, *Proceedings of 30th ICRC Merida, Mexico, (2007) Vol.1*, p. 643.
- [12] M. Casolino, *Proceedings of 30th ICRC Merida, Mexico, (2007) Vol.1*, p. 639.
- [13] A. Cappa et al, *Proceedings of 30th ICRC Merida, Mexico, (2007) Vol.1*, p. 621.
- [14] G. A. de Nolfo et al, *Proceedings of 30th ICRC Merida, Mexico, (2007) Vol.1*, p. 813.
- [15] M. B. Krainev, *Proceedings of 30th ICRC Merida, Mexico, (2007) Vol.1*, p. 465.
- [16] A. S. Asipenka et al, *Proceedings of 30th ICRC Merida, Mexico, (2007) Vol.1*, p. 629.
- [17] J. F. Cooper et al, *Proceedings of 30th ICRC Merida, Mexico, (2007) Vol.1*, p. 635.
- [18] J. T. Gosling et al, *J. Geophys. Res.* 86 (1981) 547.
- [19] E. G. Berezhko and S. N. Taneev, *Proceedings of 30th ICRC Merida, Mexico, (2007) Vol.1*, p. 799.
- [20] J. M. Clem et al, *Astrophys. J.* 464 (1996) 507.
- [21] J. W. Bieber et al, *Physical Review Letters* 83 (1999) 674.
- [22] Y. Asaoka et al, *Physical Review Letters* 88 (2002) 051101.
- [23] J. Clem and P. Evenson, *Proceedings of 30th ICRC Merida, Mexico, (2007) Vol.1*, p. 477.
- [24] O. Sternal et al, *Proceedings of 30th ICRC Merida, Mexico, (2007) Vol.1*, p. 451.
- [25] J. Casolino et al, *Proceedings of 30th ICRC Merida, Mexico, (2007) Vol.1*, p. 489.
- [26] M. Hareyama et al, *Proceedings of 30th ICRC Merida, Mexico, (2007) Vol.1*, p. 647.
- [27] A. Dragic et al, *Proceedings of 30th ICRC Merida, Mexico, (2007)*, Id 0957.
- [28] V. Okhlopkov and Y. Stozhkov, *Proceedings of 30th ICRC Merida, Mexico, (2007) Vol.1*, p. 481.
- [29] A. V. Belov et al, *Proceedings of 30th ICRC Merida, Mexico, (2007) Vol.1*, p. 473.
- [30] C. Grimani et al, *Proceedings of 30th ICRC Merida, Mexico, (2007) Vol.1*, p. 485.
- [31] J. W. Mitchell et al, *Proceedings of 30th ICRC Merida, Mexico, (2007) Vol.1*, p. 455.
- [32] I. V. Moskalenko et al, *Astrophys. J.* 565 (2002) 280.
- [33] M. Hitge and R. A. Burger, *Proceedings of 30th ICRC Merida, Mexico, (2007) Vol.1*, p. 449.
- [34] S. Miyake and S. Yanagita, *Proceedings of 30th ICRC Merida, Mexico, (2007) Vol.1*, p. 445.
- [35] R. A. Burger and P. C. Sello, *Advances in Space Research* 35 (2005) 643.
- [36] S. Usoskin et al, *Proceedings of 30th ICRC Merida, Mexico, (2007) Vol.1*, p. 459.
- [37] J. Minnie et al, *Proceedings of 30th ICRC Merida, Mexico, (2007) Vol.1*, p. 433.
- [38] P. Bobik et al, *Proceedings of 30th ICRC Merida, Mexico, (2007) Vol.1*, p. 413.
- [39] A. Shalchi et al, *Proceedings of 30th ICRC Merida, Mexico, (2007) Vol.1*, p. 409.
- [40] I. D. Palmer, *Reviews of Geophysics and Space Physics* 20 (1982) 335.
- [41] A. Shalchi and I. Kourakis, *Proceedings of 30th ICRC Merida, Mexico, (2007) Vol.1*, p. 405.
- [42] G. Gloeckler et al, *Geophys. Res. Lett.* 22 (1995) 2665.
- [43] E. Möbius et al, *J. Geophys. Res.* 103 (1998) 257.
- [44] S. Dasso et al, *Proceedings of 30th ICRC*

- Merida, Mexico, (2007) Vol.1, p. 625.
- [45] M. V. Alania et al, Proceedings of 30th ICRC Merida, Mexico, (2007) Vol.1, p. 497.
- [46] G. S. Nkosi et al, Proceedings of 30th ICRC Merida, Mexico, (2007) Vol.1, p. 429.
- [47] R. A. Burger and N. E. Engelbrecht, Proceedings of 30th ICRC Merida, Mexico, (2007) Vol.1, p. 437.
- [48] O. G. Morales and R. A. Caballero-Lopez, Proceedings of 30th ICRC Merida, Mexico, (2007) Vol.1, p. 567.
- [49] J. Gieseler et al, Proceedings of 30th ICRC Merida, Mexico, (2007), Id 0354.
- [50] M. B. Krainev and M. S. Kalinin, Proceedings of 30th ICRC Merida, Mexico, (2007) Vol.1, p. 417.
- [51] R. A. Leske et al, Proceedings of 30th ICRC Merida, Mexico, (2007) Vol.1, p. 807.
- [52] V. M. Velasco et al, Proceedings of 30th ICRC Merida, Mexico, (2007) Vol.1, p. 553.
- [53] K. G. McCracken, Proceedings of 30th ICRC Merida, Mexico, (2007) Vol.1, p. 545.
- [54] M. Laurenza et al, Proceedings of 30th ICRC Merida, Mexico, (2007) Vol.1, p. 513.
- [55] L. de Caso et al, Proceedings of 30th ICRC Merida, Mexico, (2007) Vol.1, p. 505.
- [56] M. K. Richharia and S. K. Shrivastava, 0094.
- [57] M. K. Richharia and M. L. Chauhan, Proceedings of 30th ICRC Merida, Mexico, (2007), Id 0115.
- [58] R. Modzelewska and M. V. Alania, Proceedings of 30th ICRC Merida, Mexico, (2007) Vol.1, p. 597.
- [59] A.F. Li et al, Proceedings of 30th ICRC Merida, Mexico, (2007), Id 0445.
- [60] M. Amenomori et al, Proceedings of 30th ICRC Merida, Mexico, (2007) Vol.1, p. 577.
- [61] J. Kóta et al, Proceedings of 30th ICRC Merida, Mexico, (2007) Vol.1, p. 589.
- [62] D. J. McComas and N. A. Schwadron, Geophys. Res. Lett. 33 (2006) 4102.
- [63] S. E. S. Ferreira et al, Proceedings of 30th ICRC Merida, Mexico, (2007) Vol.1, p. 857.
- [64] H. Moraal et al, Proceedings of 30th ICRC Merida, Mexico, (2007) Vol.1, p. 865.
- [65] H. Moraal et al, AIP Conf. Series,(2006) Vol.858, p. 219.
- [66] F. B. McDonald et al, Geophys. Res. Lett. 34 (2007) 5105.
- [67] A. C. Cummings and E. C. Stone, Proceedings of 30th ICRC Merida, Mexico, (2007) Vol.1, p. 827.
- [68] V. Florinski and G. P. Zank, Geophys. Res. Lett. 33 (2006) 15110.
- [69] J. R. Jokipii and J. Giacalone, Proceedings of 30th ICRC Merida, Mexico, (2007), Vol. 1, p. 851.
- [70] E. C. Stone et al, Proceedings of 30th ICRC Merida, Mexico, (2007) Vol.1, p. 831.
- [71] A. C. Cummings, E. C. Stone, and C. D. Steenberg, Astrophys. J. 578 (2002) 194.
- [72] A. C. Cummings, E. C. Stone, and C. D. Steenberg, Astrophys. J. 581 (2002) 1413.
- [73] M. Hilchenbach et al, Proceedings of 30th ICRC Merida, Mexico, (2007) Vol.1, p. 837.
- [74] A. Czechowshi et al, Proceedings of 30th ICRC Merida, Mexico, (2007) Vol.1, p. 63.
- [75] J. L. Snyman et al, Proceedings of 30th ICRC Merida, Mexico, (2007) Vol.1, p. 425.